SCIENCE CHINA
Information Sciences

• RESEARCH PAPER •

February 2014, Vol. 57 022403:1–022403:9
doi: 10.1007/s11432-013-4810-0

Remote charge scattering: a full Coulomb interaction approach and its impact on silicon nMOS FinFETs with HfO_2 gate dielectric

WEI KangLiang[1], EGLEY James[2], LIU XiaoYan[1]* & DU Gang[1]

[1]*Institute of Microelectronics, Peking University, Beijing* 100871*, China;*
[2]*GLOBALFOUNDRIES, Sunnyvale, CA* 94085*, USA*

Received October 15, 2012; accepted January 2, 2013; published online January 29, 2013

Abstract Remote charge scattering (RCS) has become a serious obstacle inhabiting the performance of ultra-thin gate oxide MOSFETs. In this paper, we evaluate the impact of RCS by treating the real-space full Coulomb interaction between remote charges and inversion carriers. A new approach that can be simply incorporated in ensemble Monte Carlo (EMC) based simulations without any variation of the standard EMC simulator is developed. The charge-carrier (c-c) interaction model is based on a particle-mesh (PM) calculation method which resolves both the long-range and short-range Coulomb interactions by solving Poisson's equation on a refined mesh. The validity of our approach is verified by three-dimensional (3-D) resistor simulations, from which the obtained doping dependence of the low-field mobility agrees well with experimental results. The proposed approach is then used to study the impact of RCS on the drive current and carrier transport properties in the channel of a 20 nm silicon (Si) nMOS FinFET with HfO_2 gate stack. We find that the influence of RCS is strongly localized in the vicinity of the remote charges and exhibits a granular nature, indicating the necessity to consider the full Coulomb interaction in RCS.

Keywords carrier transport, full Coulomb interaction, gate dielectric, high-κ, Monte Carlo (MC), FinFET, remote charge scattering (RCS)

Citation Wei K L, Egley J, Liu X Y, et al. Remote charge scattering: a full Coulomb interaction approach and its impact on silicon nMOS FinFETs with HfO_2 gate dielectric. Sci China Inf Sci, 2014, 57: 022403(9), doi: 10.1007/s11432-013-4810-0

1 Introduction

As device size aggressively shrinks to nano scale, mobility degradation with decreasing gate oxide thickness has been reported [1–3]. Remote charge scattering (RCS) due to charges in a remote region situated away from the inversion channel is identified as one of the causes responsible for the mobility lowering [2,3]. With the high-κ/metal gate used in CMOS technology, this effect becomes more and more serious. Quantification of the RCS effect has been a major problem for the past decade. Early work on this issue are mostly focused on the evaluation of RCS due to ionized impurities present in the depleted poly-gate of a MOSFET [4–12]. Also, there are other studies suggesting that the ionized impurity atoms

*Corresponding author (email: xyliu@ime.pku.edu.cn)

in a polysilicon depletion region only have moderate effects on the inversion channel mobility, and that plasmons at the poly/SiO_2 interface are the dominant remote scattering source in polysilicon ultrathin gate oxide MOSFETs [13,14]. Though controversy exists over the relative importance of RCS and interface plasmons in poly-gate thin oxide MOSFETs, the advent of high-κ/metal gate stacks in modern advanced devices introduces new RCS sources arising from the presence of charged defects in the bulk of high-κ layer or at the high-κ/SiO_2 interface [15]. In addition, the metal gate can largely suppress the influence of interface plasmons [13], which in turn further highlights the importance of RCS. Later extensive works have been devoted to the effect of RCS due to charged traps in high-κ gate stacks [16–21].

However, previous theoretical studies on RCS, either due to ionized impurities in the poly-gate or due to fixed charges in high-κ gate stacks, have mostly treated the charge-carrier (c-c) interaction in terms of approximations of a $\boldsymbol{k}$ space scattering process based on a continuum charge profile assumption, by which means only the short-range, single-particle interaction are captured, while the discrete nature of remote charges in small devices, the many-body interaction, and the variation information about the long-range carrier interaction in the transport associated with the realistic distribution of the discrete remote charges in the gate stack are lost. This situation is even more serious in modern decananometre size devices since only countable charges exist in such small devices. Kawashima et al. [6] evaluated the RCS of the real-space Coulomb interaction by analytical expressions. However, this method is questionable to suit the non-planar MOSFETs, such as FinFETs.

Actually, there are several works which have considered the real-space full Coulomb interaction [22,23] to investigate the influence of carrier-impurity (c-i) interaction for ionized impurity scattering. However, to the best of our knowledge, none has evaluated the impact of RCS by treating the real-space full Coulomb interaction between remote charges and inversion carriers. Hence, developing a method to treat the full Coulomb interaction of RCS including the location of remote charges and their granular nature is important, especially to the non-planar multi-gate MOSFETs with high-κ/metal-gate stack.

In this paper, we treat granular effects and real-space full Coulomb interaction of RCS by integrating a simple yet effective c-c interaction model with our three-dimensional (3-D) ensemble Monte Carlo (EMC) simulator. The remote charges are treated discretely and located precisely during the simulation. The full Coulomb potential, including both the long-range and the short-range components, is recovered directly from the mesh-based resolution of Poisson's equation without the necessity of adding a corrective short-range force, as is done in other methods [22,23]. The method is suitable to simulate the interaction between charges and carriers, such as RCS and the influence of discrete dopants in the MOSFET.

The remainder of this paper is organized as follows. The details and physical models of the coupled particle-mesh EMC (PM/EMC) approach are described in Section 2. The validity of this new approach is verified in Section 3 through calculation of doping dependence of the low-field mobility in 3-D silicon (Si) resistors. Then simulations are performed to evaluate the impact of RCS due to trapped charges in the high-κ (HfO_2) gate stack on a 20 nm Si nMOS FinFET, with the results presented in Section 4. Finally, our conclusions are drawn in Section 5.

2 The method

This work builds upon our previous 2-D/3-D full-band EMC simulator for Si devices [24–26], which takes into account the major scattering mechanisms including phonon, surface roughness (SR), impact ionization and ionized impurity scattering to reproduce the bulk Si velocity-field characteristic and the inversion channel universal effective mobility curves [24]. In addition, the bulk Si full-band structure obtained by the local empirical pseudo-potential method is employed in this work [25].

Realizing that the interaction between remote charges and inversion carriers is analogous to the c-c interaction in devices, we first elucidate how to include the real-space full Coulomb effects of the more general c-c interaction in the 3-D EMC simulation. Our method is based on the real-space and real-time description of the carrier's transport and at the same time abandons the corresponding $\boldsymbol{k}$ space scattering process. To achieve this, carrier interaction with charged centers should be treated as extended in both the real-space and time domain. This procedure is accomplished by tracking the trajectory of each

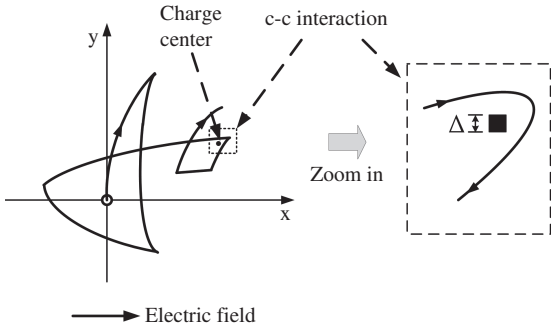

Figure 1 Diagram illustrating how the real-space trajectory (the solid line with arrows) of a particle propagating in the perturbing full Coulomb potential of a discrete charge center is tracked. We zoom in the region where the charge center exists to show how we deal with the c-c interaction more clearly.

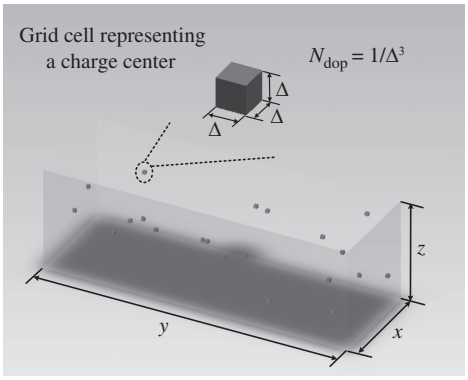

Figure 2 Charge centers are treated discretely. Each one is represented by a grid cell of size Δ, which is with uniform doping concentration $N_{\rm dop} = 1/\Delta^3$.

particle propagating in the perturbing full Coulomb potential associated with a discrete charged center configuration, which is illustrated in Figure 1. The full Coulomb field can be resolved for each charge from the mesh-based solution of Poisson's equation as long as we have considered the contribution of charged centers in the right hand side (RHS) of Poisson's equation. However, integration of the equations of motion may become inaccurate if we treat charges as ideal points, especially in the case where the charges lie close to the channel. This is because the Coulomb force of a point charge is proportional to $1/r^2$; hence, it increases dramatically as we approach closely. As a particle falls into this potential well, it is rapidly converting potential energy into kinetic energy, leading to unphysical heating of the system [23,27]. A number of alternative approaches based on a particle-particle particle-mesh (P^3M) algorithm have been developed to make corrections to the short-range force to prevent carrier heating while at the same time maintaining the accuracy of the c-c interaction as much as possible [22,23,27]. However, they necessitate additional modifications to the standard EMC method. Here we have come up with a new approach to introduce charged centers and the associated granular effects to standard EMC simulations.

In MC simulation, doping regions of a device are mostly treated as fully depleted; hence when we construct Poisson's equation of the device, the ionized dopant atoms are viewed as fixed charges, with their polarity being positive in n-type regions and negative in p-type regions. In this sense, we can get positive charges by performing donor doping and negative charges by acceptor doping. Following the proposed method, in the cell (assuming its size to be Δ) where a fixed charge should exist, a uniform doping with density $1/\Delta^3$ is performed in that specific cell to represent the charge (see Figure 2 and also the zoom in region of Figure 1). The doping type is chosen according to the polarity of the charge. If two or more charged centers should be located in the same cell, the doping density is adjusted accordingly. In this way, we can take into account the actual position of the discrete charged centers in EMC simulations. Moreover, because only a continuum doping profile in each cell is assumed, no changes are needed to the standard EMC simulator.

However, there is still special care that needs to be taken. To illustrate the issue, we have solved Poisson's equation to calculate the typical potential profiles around a fixed charge represented with a cell of different mesh sizes ranging from 0.5 nm to 2 nm and plotted them in Figure 3. For comparison, also plotted is the analytical Coulomb potential of an ideal point charge situated in the center of the cell. It is obvious to see that the calculated mesh potential coincides with the analytical Coulomb potential in the long range from the charge. However, in the short range the mesh force experienced by carriers deviates from the real Coulomb force and finally drops to zero within the cell. This is because we approximate a physically point-like charge with a cell of definite volume. The approximation can be beneficial because the potential singularity associated with a point charge is eliminated and the short-range corrective potential used to prevent carrier heating is no longer needed. However, the discrepancy between the

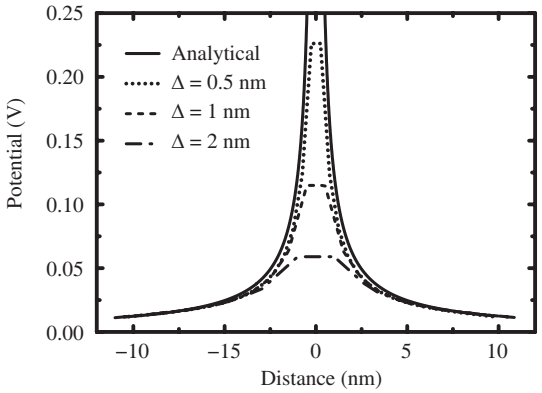

Figure 3 Calculated potential profiles (dashed lines) around a single charge represented with a cell of different mesh sizes (Δ) ranging from 0.5 nm to 2 nm and analytical Coulomb potential (solid line) of an ideal point charge situated in the center of the cell.

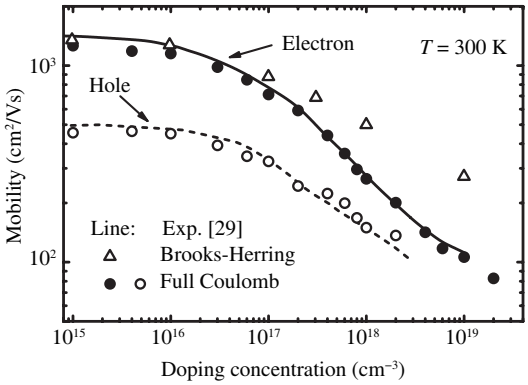

Figure 4 Comparison of low-field electron and hole mobility in bulk Si calculated with both the full Coulomb approach (solid dot for electron and circle for hole) and the conventional BH impurity scattering model (triangle) with the experimental data (solid line for electron and dashed line for hole).

mesh force and the real Coulomb force in the short range limits the validity of this approach since the latter tends to infinity when approaching the origin of the charge. Seeing from Figure 3, this discrepancy can be alleviated by refining the mesh around the fixed charge. The finer it is, the more closely it will duplicate Coulomb's force. Nevertheless, the mesh refining in turn may also hazard the accuracy of the carrier energy conservation. We resolve the trade-off of the mesh size selection by extensive tests and suggest that a Δ value between 0.5 nm and 4 nm to be an appropriate mesh size range, which is adequate for nano scale device simulations. The validation of our suggestion will be detailed in the next section. By constraining the minimum mesh size, our method is essentially analogous to the P^3M algorithm which limits the strength of the Coulomb potential for the purpose of preventing unphysical carrier heating, and is simpler.

After we have set the method for the general c-c interaction, it can be directly applied to the calculation of RCS without any modification. The only thing to be noted is that the charge-imitating-doping in the cell where remote charges situate is performed in insulator regions. Moreover, it should be pointed out that to treat RCS with a particle-point charge approach would require one to add the image force to the force on the particle due to the differing dielectric constants between silicon and the dielectric, while using our approach of Poisson's solution, automatically includes this [28].

3 Verification

As mentioned above, the present approach can also be suitable to simultaneously take into account all kinds of carrier interactions with the charge centers including ionized impurities. This provides a simple way for the verification of our approach. By using the full Coulomb approach to substitute the conventional ionized impurity scattering (such as Brooks-Herring (BH) model) in the EMC simulation, the doping dependence of the low-field electron and hole mobility is simulated and plotted in Figure 4. The Si resistor with various doping concentration is simulated by the 3-D MC simulator.

According to its position, each ionized impurity is represented by a cell with a uniform doping concentration $1/\Delta V$, assuming the cell volume to be ΔV. The total number of impurities ($N_{\rm im}$) in a resistor is determined by the product of its volume V and the background doping concentration $N_{\rm dop}$, i.e. $N_{\rm im} = N_{\rm dop} \times V$, and all of the impurities are randomly and discretely distributed in the whole resistor region. To maintain reasonable computing efficiency, the size of the resistor, i.e. its volume V, is adjusted according to the background doping concentration $N_{\rm dop}$ so that the correct number of impurity atoms, $N_{\rm im}$, are included in the simulation. Moreover, to keep the simulation accuracy, the mesh size Δ is also carefully tuned so that the total number of impurities does not exceed a specific ratio of the

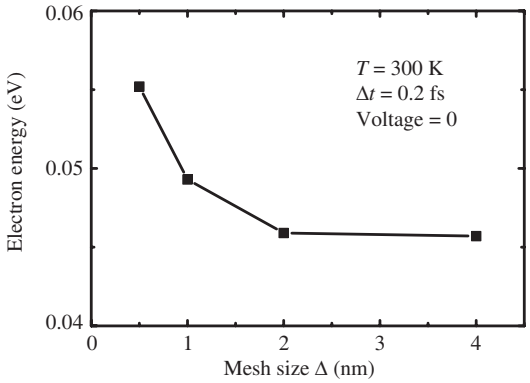

Figure 5 Influence of the mesh size Δ on the accuracy of electron energy conservation at 300 K. The voltage applied to resistors is set to zero and the self-consistent simulation time step is 0.2 fs.

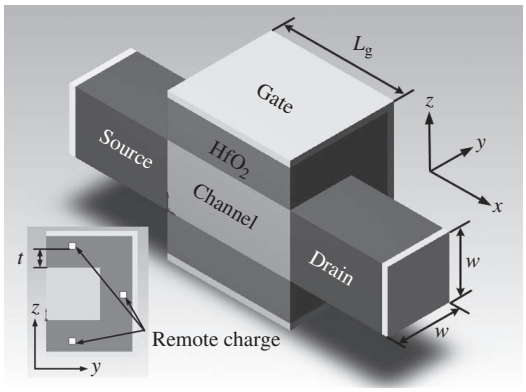

Figure 6 Schematic structure of the Si nMOS FinFET. The existing remote charges in the gate dielectric are shown, with the distance to Si/HfO_2 interface denoted by t.

total number of mesh cells. This ratio is chosen to be 1/1000 in this work based on the reasoning that the number of activated impurity atoms generally will not exceed 1/1000 of the number of Si atoms. Based on this hypothesis, we can derive a relation between the mesh size Δ and the background doping concentration $N_{\rm dop}$ as $\Delta \leqslant \sqrt[3]{10^{18}/N_{\rm dop}}$, where the units of Δ and $N_{\rm dop}$ are nanometer and per cubic centimeter, respectively.

Two metallic contacts are placed at the two ends of each resistor, and periodic boundary conditions are used at these contacts. The voltage applied to the resistor varies with the resistor length so as to apply a constant driving field in the carrier propagation direction. Self-consistent simulation is employed and the time step Δt is 0.2 fs. For each doping concentration, we can get a stable velocity distribution in the resistor from the Monte Carlo simulation, from which an average velocity of the electron or hole can be obtained. The average velocity depends on the electric field ($\boldsymbol{E}$) applied. Here we first use $E = 1$ kV/cm, and get the average velocity v. We then shift the electric field by a small amount ΔE (e.g. 500 V/cm) and get the corresponding average velocity $v + \Delta v$. The mobility (μ) can be calculated simply from $\mu = \Delta v/\Delta E$.

Figure 4 shows the calculated low-field electron and hole mobility in bulk Si as a function of the doping concentration and the experimental data is also plotted for comparison [29]. Also shown are the results of electron mobility obtained with the conventional BH impurity scattering model. It is obvious that the results using BH model strongly overestimate the mobility in the heavily doped regime since the many-body dynamic screening and the multi-ion scattering effects that dominate the transport in this doping regime cannot be included in the BH model. The results using the full Coulomb approach agree well with the experimental data at very high doping concentrations, up to 2×10^{19} cm^{-3}, which gives us confidence in introducing the full Coulomb model to the evaluation of the interaction between carriers and charge centers. To further give a reliable assessment of the influence of the mesh size Δ on the accuracy of the carrier energy conservation, we have performed simulations with the voltage applied to the resistors set to zero. The average electron equilibrium energy at 300 K as a function of mesh size Δ is plotted in Figure 5. It is observed that for a mesh size larger than 0.5 nm, there is no, or only slight, electron heating (less than 35% of the thermal kinetic energy, $k_{\rm B}T$), which can be totally neglected since it will not influence the transport in a significant way, as evidenced by our reproduction of the low-field mobility in Figure 4. This observation justifies our former suggestion on the proper mesh size range in the last section.

4 Full Coulomb effects of RCS on FinFETs

Using the proposed full Coulomb approach, we have further investigated the impact of the granular effects of RCS on a Si nMOS FinFET, of which the schematic device structure is shown in Figure 6. The gate

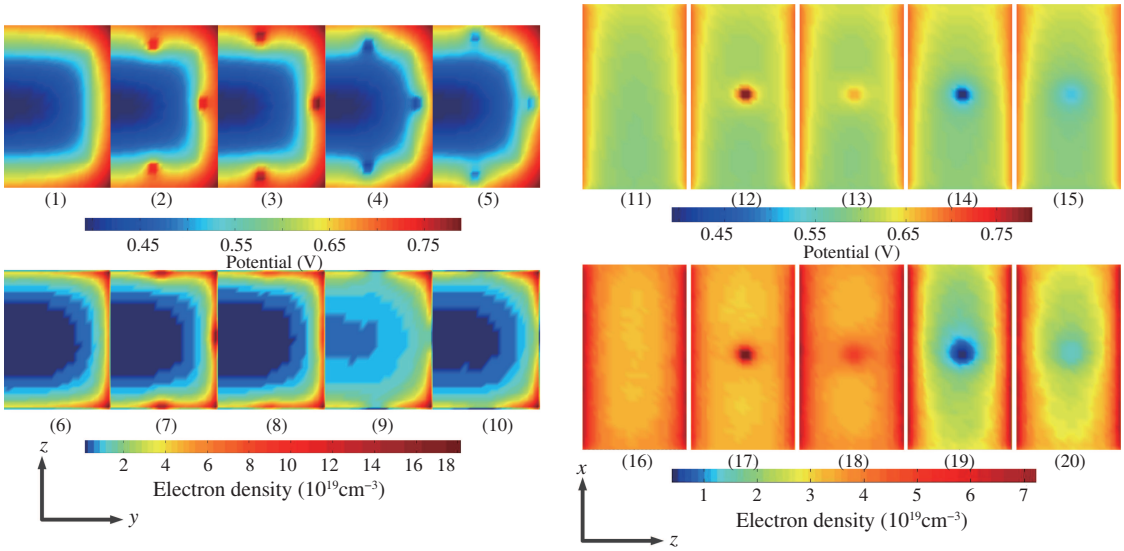

Figure 7 Potential and electron density profiles (1)–(10) in the y-z plane cut in the middle of the channel (11)–(20) in the x-z plane at the Si/HfO_2 interface. Different charge polarities and distance to the Si/HfO_2 interface are considered. $V_{gs} = 0.8$ V, $V_{ds} = 50$ mV. The charge polarity and distance to interface t is: (1), (6), (11), (16) no charge; (2), (7), (12), (17) positive, $t = 0.25$ nm; (3), (8), (13), (18) positive, $t = 1$ nm; (4), (9), (14), (19) negative, $t = 0.25$ nm; (5), (10), (15), (20) negative, $t = 1$ nm.

length $L_g = 20$ nm, channel cross-sectional size is 10×10 nm^2, and the length of source and drain regions is 15 nm. The gate dielectric is a layer of 6 nm thick HfO_2, and its permittivity is carefully chosen so that the effective oxide thickness EOT = 1 nm. The source and drain is n-doping with a uniform density 10^{20} cm^{-3}, and the channel is left intrinsic. All electrodes are assumed to be metallic. Remote charges are introduced to the device by putting a positive or negative charge on each side of the MOSFET gate dielectric (corresponding to a sheet charge density of 5×10^{11} cm^{-2}). Charges with different distance t from the Si/HfO_2 interface are considered in our simulation. For the purpose of accuracy, mesh size around the remote charges is chosen to be 0.5 nm. Because we focus on evaluating the effects of RCS, ionized impurity scattering in the source and drain regions is still considered using the conventional BH model.

Figure 7 shows the potential and electron density profiles in the y-z plane cut in the middle of the channel and in the x-z plane at the Si/HfO_2 interface with positive or negative charges in the gate dielectric at $V_{gs} = 0.8$ V and $V_{ds} = 50$ mV. The case where there is no charge in the dielectric is also shown for comparison. It is clearly seen that the profiles are significantly reshaped by charges present in the dielectric, especially when they lie close to the interface. Furthermore, the influence of RCS is strongly localized to where the charges are located, indicating the important role that the charge granularity plays in RCS.

Figure 8 plots the impact of discrete remote charges on the drive current of the FinFET. Compared with the case where there is no charge in the dielectric, positive charges can moderately increase the current, while negative charges degrade the drain current significantly. This can be explained with the corresponding electron density profile and drift velocity distribution shown in Figure 9 and Figure 10, respectively. From Figure 9 we see that the channel electron density in the vicinity of the remote charge is substantially influenced, as can also be observed from the 2-D density distribution in Figure 7. When positive charges exist, the electron density increases; while when negative charges exist, the electron density decreases. This indicates that the charges in the dielectric will exert a flatband shift, and consequently a threshold voltage shift, on the MOSFET, which is clearly reflected in our full Coulomb approach. Figure 10 shows the drift velocity distribution in the channel. At low drain bias ($V_{ds} = 0.05$ V), we see that the charge polarity makes differences. This is because the positive charge is well screened by the electrons accumulating in the channel, and its influence is restricted to the vicinity of the charge. However, the impact of the negative charge extends across the whole channel due to the imperfection of screening. For

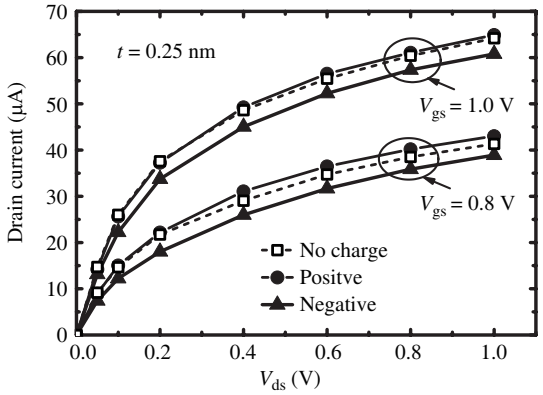

Figure 8 I_{ds}-V_{ds} curves of Si nMOS FinFET with positive and negative charges in the gate dielectric at distance of 0.25 nm from interface. The case there is no charge in the dielectric (w/o RCS) is also shown.

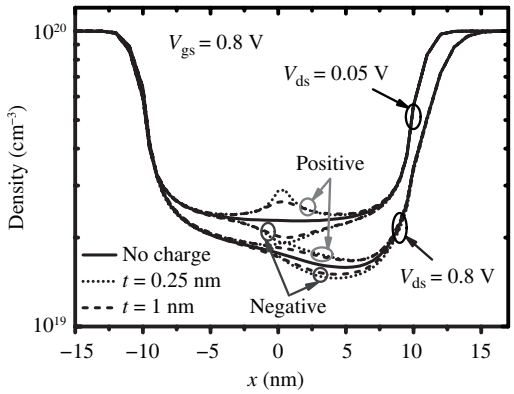

Figure 9 Average electron density distribution of Si nMOS FinFET with positive and negative charges in the gate dielectric at $V_{gs} = 0.8$ V, $V_{ds} = 50$ mV and 0.8 V.

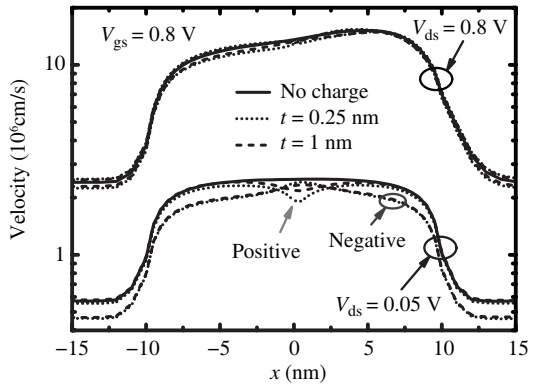

Figure 10 Average electron drift velocity distribution of Si nMOS FinFET with positive and negative charges in the gate dielectric at $V_{gs} = 0.8$ V, $V_{ds} = 50$ mV and 0.8 V.

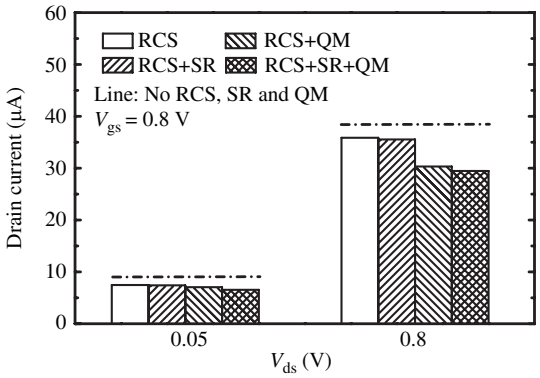

Figure 11 The relative importance of RCS, SR and QM effects on the drain current at $V_{gs} = 0.8$ V, $V_{ds} = 50$ mV and 0.8 V. The lines indicate the case where no RCS, SR or QM is included.

the reason described above, only the electron drift velocity around the positive charge is decreased due to the Coulomb interaction, while the velocity in the whole channel diminishes because of the Coulomb interaction from the negative charge. At high drain bias ($V_{ds} = 0.8$ V), the impact of RCS on the velocity is negligible for the much higher velocity in the channel. This coincides with the regime where Coulomb scattering mainly takes effect. Thus negative charges lead to decreased electron channel density and velocity, which results in decreased drain current; while for positive charges, the increased carrier density and decreased velocity offset each other, resulting in almost no change or a moderate increase in the conduction current.

Figure 11 summarizes the relative importance of RCS (negative charges only), SR and quantum mechanical (QM) effects on the drain current. The QM effect is considered in the effective potential scheme [26]. It can be seen that RCS plays a more important role in affecting the drain current than SR scattering. On the other hand, the QM effect can also have a significant influence due to the small feature size of the device with a 10×10 nm^2 cross section.

Finally, it is worth noting that, compared with conventional RCS models based on scattering rates, the small mesh size used to accurately calculate the mesh force does not exert much extra load on the computational resources since mesh refining is only performed in the vicinity of fixed charges. In this work, mesh refining is mostly in the insulator region and induces a computation increase of no more than 20%. In fact, the suggested mesh spacing range is not so exceedingly aggressive when considering devices of decananometre size.

5 Conclusion

A new approach that incorporates the full Coulomb interaction between carriers and charge centers has been proposed and verified against experiments. This method has the advantage that it can be simply implemented without any modification of the standard EMC simulator, and therefore serves as a good alternative to the conventional P^3M algorithm. By applying the proposed method to a 20 nm gate length FinFET, we conclude that: (i) In small devices, even a single charge in the gate insulator can have significant impact on the electrostatics and carrier transport in the channel, while the influence of surface roughness is relatively negligible. (ii) Different charge polarity has distinct effects. It is quantitatively shown that positive charges can moderately increase the conduction current, while negative charges severely decrease it. (iii) The impact of RCS is strongly localized in the vicinity of the charge. This granular nature of RCS introduces another variation source to the conduction current, which makes the consideration of full Coulomb interaction in RCS necessary in the future work on this subject.

Acknowledgements

This work was supported by National Key Basic Research Program of China (Grant No. 2011CBA00604).

References

1 Xiang Q, Yeap G, Bang D, et al. Performance and reliability of sub-100 nm MOSFETs with ultra thin direct tunneling gate oxides. In: Symposium on VLSI Technology Technical Digest. Piscataway: IEEE Press, 1998. 160–161
2 Krishnan M S, Chang L, King T J, et al. MOSFETs with 9 to 13 Å thick gate oxide. In: International Electron Devices Meeting Technical Digest. Piscataway: IEEE Press, 1999. 241–244
3 Takagi S, Takayanagi M. Experimental evidence of inversion-layer mobility lowering in ultrathin gate oxide metal-oxide-semiconductor field-effect-transistors with direct tunneling current. Jpn J Appl Phys, 2002, 41: 2348–2352
4 Krishnan M S, Yeo Y C, Lu Q, et al. Remote charge scattering in MOSFETs with ultra-thin gate dielectrics. In: International Electron Devices Meeting Technical Digest. Piscataway: IEEE Press, 1998. 571–574
5 Yang N, Henson W K, Hauser J R, et al. Estimation of the effects of remote charge scattering on electron mobility of n-MOSFETs with ultrathin gate oxides. IEEE Trans Electron Dev, 2000, 47: 440–447
6 Kawashima I, Kamakura Y, Taniguchi K. Ensemble Monte Carlo/molecular dynamics simulation of gate remote charge effects in small geometry MOSFETs. In: International Electron Devices Meeting Technical Digest. Piscataway: IEEE Press, 2000. 113–116
7 Saito S, Torii K, Hiratani M, et al. Improved theory for remote-charge-scattering-limited mobility in metal-oxide-semiconductor transistors. Appl Phys Lett, 2002, 81: 2391–2393
8 Esseni D, Abramo A. Modeling of electron mobility degradation by remote Coulomb scattering in ultrathin oxide MOSFETs. IEEE Trans Electron Dev, 2003, 50: 1665–1674
9 Gamiz F, Roldan J B, Carceller J E, et al. Monte Carlo simulation of remote-Coulomb-scattering-limited mobility in metal-oxide-semiconductor transistors. Appl Phys Lett, 2003, 82: 3251–3253
10 Gamiz F, Fischetti M V. Remote Coulomb scattering in metal-oxide-semiconductor field effect transistors: Screening by electrons in the gate. Appl Phys Lett, 2003, 83: 4848–4850
11 Lucci L, Esseni D, Loo J, et al. Quantitative assessment of mobility degradation by remote coulomb scattering in ultra-thin oxide MOSFETs: Measurements and simulations. In: International Electron Devices Meeting Technical Digest. Piscataway: IEEE Press, 2003. 463–466
12 Ishihara T, Koga J, Matsuzawa K. Modeling of screening effect on remote Coulomb scattering due to gate impurities by nonuniform free carriers in poly-Si gate. J Appl Phys, 2007, 102: 073702
13 Fischetti M V. Long-range Coulomb interactions in small Si devices—part II: Effective electron mobility in thin-oxide structures. J Appl Phys, 2001, 89: 1232–1250
14 Chen M J, Chang S C, Kuang S J, et al. Temperature-dependent remote-Coulomb-limited electron mobility in n^+-polysilicon ultrathin gate oxide nMOSFETs. IEEE Trans Electron Dev, 2011, 58: 1038–1044
15 Casse M, Thevenod L, Guillaumot B, et al. Carrier transport in HfO_2/metal gate MOSFETs: Physical insight into critical parameters. IEEE Trans Electron Dev, 2006, 53: 759–768
16 Ono M, Ishihara T, Nishiyama A. Influence of dielectric constant distribution in gate dielectrics on the degradation of electron mobility by remote Coulomb scattering in inversion layers. IEEE Trans Electron Dev, 2004, 51: 736–740
17 Lujan G S, Magnus W, Ragnarsson L A, et al. Modeling mobility degradation due to remote Coulomb scattering from dielectric charges and its impact on MOS device performance. Microelectron Reliab, 2005, 45: 794–797

18 Saito S, Torii K, Shimamoto Y, et al. Remote-charge-scattering limited mobility in field-effect transistors with SiO_2 and Al_2O_3/SiO_2 gate stacks. J Appl Phys, 2005, 98: 113706
19 Barraud S, Thevenod L, Casse M, et al. Modeling of remote Coulomb scattering limited mobility in MOSFET with HfO_2/SiO_2 gate stacks. Microelectron Eng, 2007, 84: 2404–2407
20 Toniutti P, Palestri P, Esseni D, et al. Revised analysis of the mobility and I_{ON} degradation in high-κ gate stacks: surface optical phonons vs. remote Coulomb scattering. In: Proceedings of the 38th European Solid-State Device Research Conference. Piscataway: IEEE Press, 2008. 246–249
21 Poli S, Pala M G, Poiroux T. Full quantum treatment of remote Coulomb scattering in silicon nanowire FETs. IEEE Trans Electron Dev, 2009, 56: 1191–1198
22 Gross W J, Vasileska D, Ferry D K. Ultrasmall MOSFETs: The importance of the full Coulomb interaction on device characteristics. IEEE Trans Electron Dev, 2000, 47: 1831–1837
23 Alexander C, Roy G, Asenov A. Random-dopant-induced drain current variation in nano-MOSFETs: A three-dimensional self-consistent Monte Carlo simulation study using "ab initio" ionized impurity scattering. IEEE Trans Electron Dev, 2008, 55: 3251–3258
24 Du G, Liu X, Xia Z, et al. Monte Carlo simulation of p- and n- channel GOI MOSFETs by solving the quantum Boltzmann equation. IEEE Trans Electron Dev, 2005, 52: 2258–2264
25 Wei K L, Liu X Y, Du G, et al. Simulation of carrier transport in heterostructures using the 2D self-consistent full-band ensemble Monte Carlo method. J Semiconductors, 2010, 31: 084004
26 Du G, Zhang W, Wang J, et al. Study of 20 nm bulk FinFET by using 3D full band Monte Carlo method with effective potential quantum correction. In: Proceedings of the 10th International Conference on Solid-State and Integrated Circuit Technology. Piscataway: IEEE Press, 2010. 1952–1954
27 Alexander C, Watling J, Asenov A. Numerical carrier heating when implementing P^3M to study small volume variations. Semicond Sci Technol, 2004, 19: S139–S141
28 Jackson J D. Classical Electrodynamics. 3rd ed. San Francisco: John Wiley & Sons, 1998
29 Taur Y, Ning T H. Fundamentals of Modern VLSI Devices. 2nd ed. London: Cambridge University Press, 2009